Surface-Modified Biochar in a Bioretention System for *Escherichia coli* Removal from Stormwater

Abbe Y.T. Lau[a], Daniel C.W. Tsang[a,*], Nigel J.D. Graham[b], Yong Sik Ok[c], Xin Yang[d], Xiang-dong Li[a]

Graphical Abstract:

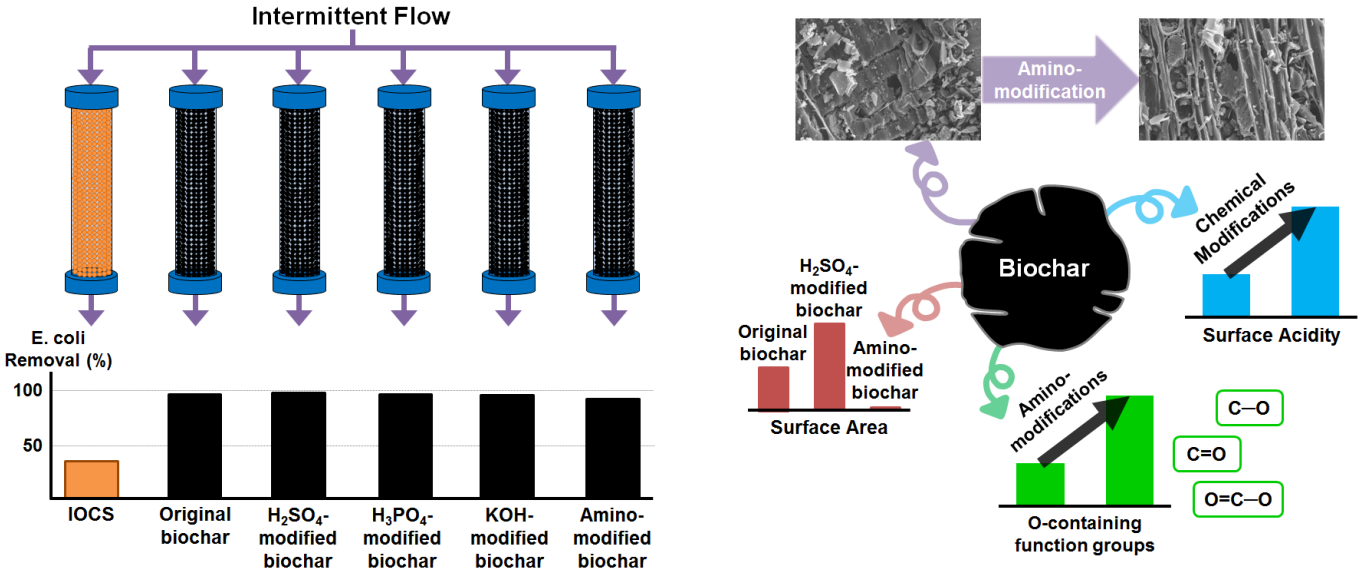

Highlights:

- Biochar was an effective bioretention filter media for *E. coli* removal
- H_2SO_4-modified biochar improved *E. coli* retention and reduced remobilization
- H_2SO_4-modification doubled surface area of original biochar
- Amino-modification enriched O-containing group density and reduced porosity
- Biochar properties played a significant role in fate and transport of *E. coli*

Surface-Modified Biochar in a Bioretention System for *Escherichia coli* Removal from Stormwater

Abbe Y.T. Lau[a], Daniel C.W. Tsang[a,*], Nigel J.D. Graham[b], Yong Sik Ok[c], Xin Yang[d], Xiang-dong Li[a]

[a] *Department of Civil and Environmental Engineering, The Hong Kong Polytechnic University, Hung Hom, Kowloon, Hong Kong, China.*

[b] *Department of Civil and Environmental Engineering, Imperial College London, South Kensington Campus, London SW7 2AZ, UK.*

[c] *Korea Biochar Research Center & School of Natural Resources and Environmental Science, Kangwon National University, Chuncheon 24341, Korea.*

[d] *School of Environmental Science and Engineering, Sun Yat-sen University, Guangzhou 510275, China.*

[*] Corresponding author: e-mail address: dan.tsang@polyu.edu.hk; tel.: +852 2766 6072; fax: +852 2334 6389.

Abstract

Bioretention systems have been recommended as one of the best management practices for low impact development for water recycling/reuse systems. Although improvement of the stormwater quality has been reported regarding pollutants eliminations such as suspended solids and heavy metals, a substantial removal of indicator bacteria is required for possible non-potable reuse. This study investigated the efficiency of wood biochar with H_2SO_4-, H_3PO_4-, KOH-, and amino-modifications for *E. coli* removal from synthetic stormwater under intermittent flow. The H_2SO_4-modified biochar showed a specific surface area of 234.7 $m^2\ g^{-1}$ (approximately double the area of original biochar), whereas a substantial reduction in surface area was found with amino-modified biochar. The *E. coli* removal (initial concentration of $0.3\text{-}3.2\times10^6$ CFU mL^{-1}) by modified biochars as filter media was very promising with, for example, over 98% removal efficiency in the first 20 pore volumes of stormwater infiltration and over 92% removal by the end of the second infiltration cycle. Only a small portion of *E. coli* attached on the modified biochars (< 0.3%, except KOH- and amino-modified biochars) was remobilized during the drainage phase of intermittent flow. The high removal capacity and stability against drainage were attributed to the high surface area, porous structure, and surface characteristics (e.g. hydrophobicity and O-containing functional groups) of the biochars. Thus, the H_2SO_4-modified biochar appeared to give the best treatment performance.

Keywords: bacteria removal; bioretention systems; designer biochar; intermittent flow; stormwater harvesting.

1. Introduction

In recent years, substitution, regeneration, and reduction are suggested as complementary approaches for improving water productivity and ecosystem sustainability (Grant et al., 2012). The substitution approach uses lower-quality water (such as reclaimed wastewater) to replace higher-quality drinking water for non-potable municipal, industrial, and agricultural activities. Although the Pearl River Delta region is increasingly water-stressed as a result of industrialization, urbanization, and population growth in industrial and commercial centres (Civic Exchange, 2011), Hong Kong relies heavily on the imported water from the Dongjiang River (70-80% of total supply) because of insufficient local yield from rainfall capture (HK WSD, 2016). Hence, rainwater harvesting systems have been implemented in public housings, shopping centres, and government buildings in Hong Kong, which is estimated to save up to 50% of water for landscape irrigation in the neighbourhood (HK GBC, 2014). In addition, stormwater is currently collected and discharged into receiving water bodies via separate drainage systems (HK DSD, 2013), which can potentially be harvested for non-potable uses with an adoption of low impact development approach as an alternative to traditional stormwater drainage design in new town development.

Bioretention systems are passive and chemical-free methods for capturing and treating stormwater at source (CIRIA, 2015; Water by Design, 2014), which have proved efficient in reducing runoff volumes and concentrations of suspended solids, total nitrogen and phosphorus, as well as heavy metals (Davis et al., 2009; Roy-Poirier et al., 2010; Stagge et al., 2012). For removal of microorganisms, the performance of bioretention is more variable depending on the watershed characteristics, surrounding hydrogeology, etc. Pathogen concentrations in surface runoff vary significantly throughout the year from 10^1 to 10^6 colony forming units (CFU) per 100 mL of stormwater depending on the land use and catchment area/type (Lundy et al., 2012). Faecal indicator bacteria in urban runoff, such as *Escherichia*

62 *coli* (*E. coli*) and total coliforms, are identified as one of the leading causes of impairments to
63 surface waters (Arnone and Walling, 2007; Gaffield et al., 2003), as their presence indicates
64 the likelihood of contamination by viruses, protozoans, and pathogenic bacteria that may
65 cause public waterborne illnesses. A recent study has suggested that viral health risks
66 associated with the use of harvested urban stormwater for crop irrigation would be deemed
67 unacceptable based on the recommendations of the World Health Organization (Lim et al.,
68 2015).

69 Continued research on improvements to the filter media is needed to enhance the
70 performance of bioretention systems for bacteria removal from stormwater. Biochar, a
71 carbon-dense solid residue produced from biomass pyrolysis, has shown a good potential as
72 bioretention media for improving *E. coli* removal (Abit et al., 2012; Bolster and Abit, 2012).
73 Recent studies have provided a solid scientific foundation and promising evidence for
74 utilizing biochar in the bioretention filter media for removing bacteria from stormwater in the
75 co-presence of natural organic matter and throughout intermittent flows between storm events
76 (Mohanty et al, 2013; Mohanty et al., 2014). However, the effectiveness appears to vary with
77 the qualities and properties of the biochar (Mohanty and Boehm, 2015). On top of these
78 findings, this study endeavours the post-synthesis chemical modifications to tailor both
79 physical and chemical properties of biochar and examine their influences on *E. coli* removal.
80 Our findings are expected to inform the design of engineered biochar and enhance the
81 technical feasibility of biochar utilization in bioretention applications.

82 The adsorption capacity of biochar is widely recognized to depend on its
83 physicochemical characteristics (Ahmad et al., 2016; Beiyuan et al., 2016; Fang et al., 2016;
84 Zhang et al., 2015). In addition to feedstock types and pyrolysis conditions, both the physical
85 characteristics (e.g., surface area and pore size distribution) and surface chemistry (e.g.,
86 functional group density and point of zero charge) of biochar can be tailored by physical or

chemical activations (Rajapaksha et. al, 2016a; 2016b). For instance, H_3PO_4-, KOH-, and H_2SO_4-modifications of biochar were found to extensively increase the microporosity and surface area as well as enriched the density of oxygen-containing functional groups (Lin et al., 2012; Liu et al., 2008; Rajapaksha et. al, 2016a; Tsang et al., 2007). In addition, amino moieties chemically bonded onto biochars enabled strong surface complexation for contaminant immobilization (Yang and Jiang, 2014). Thus, chemically-modified biochar as a filter media in bioretention systems may promote the bacteria removal from stormwater.

This study has evaluated the *E. coli* removal efficiency of four surface-modified biochars, specifically, an amino-modified biochar (AB), a KOH-modified biochar (KB), a H_3PO_4-modified biochar (PB) and a H_2SO_4-modified biochar (SB), in comparison to an original biochar (BC) in a simplified bioretention column under intermittent flows that imitate real storm events. The engineered biochars were comprehensively characterized in terms of surface area and pore size distribution (BET and BJH analysis of nitrogen gas adsorption), density of acidic/alkaline groups (Boehm's titration), microscopic imaging with elemental mapping (scanning electron microscopy/energy dispersive spectroscopy, SEM/EDS), and identification of surface functional groups (X-ray photoelectron spectroscopy, XPS) for elucidating the observed performance in bacteria removal.

2. Materials and Methods

2.1. Synthetic Stormwater

Synthetic stormwater solutions were prepared using deionized water and the following salts with reference to recent studies (Mohanty et al., 2013; 2014; Mohanty and Boehm, 2015): 5.1 mM NaCl, 0.75 mM $CaCl_2$, 0.0075 mM $MgCl_2$, 0.33 mM Na_2SO_4, 1 mM $NaHCO_3$, 0.072 mM $NaNO_3$, 0.072 mM NH_4Cl, and 0.016 mM Na_2HPO_4. The pH was adjusted using either 0.1 M HCl or 0.1 M NaOH to 7.0 ± 1. All chemicals were purchased from Sigma-

Aldrich. The solutions were autoclaved (121 ^{o}C, 100 kPa, 30 min) before use. Escherichia coli K12 (ATCC 10798) was selected as the model bacteria because of the higher persistence of gram-negative, rather than gram-positive, bacteria, and it was cultured as described in previous studies (Mohanty et al., 2013; 2014). Tryptone Soya Agar (TSA) and Tryptone Soya Broth (TSB) were acquired from Oxoid (UK). A TSA plate, streaked with a loop of preserved strains (stored in 25% glycerol at -80 ^{o}C) was incubated at 37 ^{o}C for 24 h. A single colony was transferred into 20 mL TSB and incubated at 37 ^{o}C for 8 h. A 20 μL quantity of the culture was transferred to the second batch of 20 mL TSB and incubated at 37 ^{o}C for 16 h. The harvested culture was centrifuged at 4000 rpm for 10 min. To remove the growth media, the pellet was rinsed with phosphate buffer saline twice. The cells were pelletized and re-suspended in synthetic stormwater to achieve a suspension of 0.3-3.2×10^{6} CFU mL^{-1}. The bacterial suspension was conditioned with stormwater at 4 ^{o}C for 16-18 h and warmed to room temperature in a water bath immediately before the experiments.

2.2. Bioretention Filter Media

In typical bioretention systems, surface runoff gradually percolates through the filter layer (i.e., bioretention soil), the transition layer, and drainage layer, and then passes via underlying perforated pipes to a storage tank before reuse. In order to cater for the high rainfall intensity in Hong Kong due to its subtropical climate (average annual rainfall of 2400 mm), acid-washed Ottawa sand (AWS) and iron oxide-coated sand (IOCS) were used as the filter media. The corresponding preparation methods are described in the Supplementary Information. The biochar (supplied by Kadoorie Farm and Botanic Garden in Hong Kong) was produced from forestry wood waste (*Acacia confusa* and *Celtis sinensis*) by slow pyrolysis up to 700 ^{o}C for at least 15 h. The biochar was ground and sieved to be below 1.18 mm before use.

The H_3PO_4- and KOH-modified biochars were prepared following the methods by Lin et al. (2012), and the H_2SO_4-modified biochar was prepared according to Liu et al. (2012). Briefly, original biochar was heated and stirred with either 1 M H_3PO_4 or 0.1 M KOH at 90 ^oC, or with 10% H_2SO_4 (v/v) at 60-70 ^oC for 1 h, then cooled down to room temperature. The biochar was filtered and rinsed using deionized water until the pH of the eluate was approximately neutral. The acid-/alkali-modified biochar was dried at 60 ^oC for 24 h. The amino-modification was conducted following the method by Yang and Jiang (2014). Briefly, original biochar was stirred with concentrated H_2SO_4 and concentrated HNO_3 in a water-ice bath for 2 h and then warmed to room temperature. The solid was filtered and rinsed with deionized water and subsequently isopropanol, and then dried at 90 ^oC for 24 h to remove isopropanol. The dried biochar was stirred with deionized water and 15 M ammonium hydroxide for 15 min, followed by addition of $Na_2S_2O_4$ and stirring for another 20 h. Then, 2.9 M acetic acid was added and stirred for 15 min. After 5-h reflux at 100 ^oC, the suspension was cooled to room temperature, filtered, and washed with deionized water and isopropanol. Finally, the amino-modified biochar was dried at 90 ^oC overnight.

2.3. Characterization of Original/Modified Biochars

The surface acidic and basic groups of biochars were determined using Boehm's titration method (Boehm, 1994). Briefly, 0.1 g sample of original biochar, KB, or PB was added to 10 mL of 0.05 M HCl, $NaHCO_3$, NaOH, and Na_2CO_3, respectively, while for the SB and AB samples a mass of 0.2 g and 0.4 g, respectively, was used instead. The samples were equilibrated for 24 h and filtered. Each filtrate was added with excess HCl to ensure the complete neutralization of bases, followed by back titration with NaOH using an auto-titrator (AT 400 and APB 410, Kyoto Electronics). The specific surface area (Brunauer–Emmett–Teller, BET) and pore volume distribution (Barrett–Joyner–Halenda, BJU) of biochars were

determined from N_2 adsorption-desorption isotherms at 77 K using a gas sorption analyser (NOVA-1200, Quantachrome Corporation). The micropore volume and surface area were calculated by the t-plot method.

The morphology of biochar samples was observed with a scanning electron microscope (SEM, Model JSM-6380LV, JEOL) equipped with an energy-dispersive spectrometer at 20 kV (EDS, INCA X-sight, Oxford Instruments). Thermogravimetric analysis was performed using a thermogravimetric analyser (TGA, STA 449C Jupiter, Netzch) with nitrogen stripping gas at a heating rate of 10 ^{o}C min^{-1}. The XPS spectra of the biochars were obtained using a PHI Quantera spectrometer (USA). The binding energies were referenced to the C1s peak at 284.6 eV for calibration. The deconvolution of XPS peaks was conducted using by XPSPEAK (version 4.1) software with % Gaussian-Lorentzian of 30% and Shirley background subtraction.

2.4. Bioretention Column Experiments

Each glass chromatography column (Kontes, 2.5-cm diameter, 15-cm length) was packed with a mixture of AWS (90% w/w), IOCS (5% w/w), and biochar (5% w/w). All filter media were autoclaved (121 ^{o}C, 100 kPa, 20 min) before dry-packing. The whole column set-up, including tubing, was sterilized with 70% ethanol prior to packing. The pore volume (PV) was estimated to be 28.5 mL by subtracting the weight of the dry-packed column from the completely saturated column. To remove air from pores between packed filter media grains and equilibrate the filter media, 20 PV of sterile synthetic stormwater was injected upward through the columns before the experiments (Mohanty et al., 2013; 2014).

In order to imitate real storm events, there were three phases for the column experiments: an adsorption phase in saturated conditions, a desorption phase in saturated conditions before drainage, and a desorption phase in unsaturated conditions after drainage. About 10 PV of

187 synthetic stormwater with E. coil concentration of 0.3-3.2×10^6 CFU mL^{-1}, followed by 10 PV
188 of sterile synthetic stormwater, was pumped upward at 2 mL min^{-1} from the bottom inlet.
189 Subsequently, the flow was stopped and then the column was turned over (180°) for draining
190 the pore water by gravity for 20 min (i.e., consistent with inflow direction) during the
191 drainage phase. After the gravity drainage, the drained column was returned to its original
192 direction and sealed for 16 h. 5 PV of sterile synthetic stormwater was then injected upward
193 through the column. The cycle of infiltration and drainage phases was repeated, as illustrated
194 in Figure S1 (Supplementary Information). The effluent samples were regularly collected
195 every 1 PV, and the bacterial concentrations (CFU mL^{-1}) in the influent (C_o) and effluent (C)
196 samples were enumerated by spread plating techniques using three decimal dilutions.
197 Duplicate plates with 30 to 300 CFU per plate were used to obtain an average *E. coli*
198 concentration. All experiments were conducted in duplicate.
199

200 **3. Results and Discussion**

201 *3.1. Original and modified biochars*

202 As shown in Table 1, both H_3PO_4- and H_2SO_4-modifications increased the specific
203 surface area (S_{BET}) and total pore volume (V_{total}) of original biochar from 137.0 m^2 g^{-1} and
204 0.0622 m^3 g^{-1} to 160.9 m^2 g^{-1} and 0.0733 m^3 g^{-1} for PB, or 230.6 m^2 g^{-1} and 0.1052 m^3 g^{-1} for
205 SB, respectively, which is favourable for *E. coli* adsorption. The wet sulphuric oxidation
206 process may lead to the considerable creation and enlargement of pores via carbon
207 gasification, accounting for a significant increase in the specific surface area and total pore
208 volume (Foo et al., 2012; Guo et al., 2005). However, there was a slight decrease in the
209 corresponding values for KB (113.8 m^2 g^{-1} and 0.0557 m^3 g^{-1}) and a substantial reduction
210 with AB (2.63 m^2 g^{-1} and 0.0032 m^3 g^{-1}). This may have resulted from the remarkable
211 destruction of pores during highly oxidative acidic modification (Figure S2) and pore

blockage by the amino functional groups grafted onto AB, which were similarly observed in the latest studies (Kang et al., 2016; Li et al., 2016).

The SEM images show porous surface structures of the biochars (Figure 1), which have no drastic change in their porous characteristics after H_2SO_4-, H_3PO_4- and KOH-modifications. The pore structures of SB, PB, and KB were largely composed of micropores with the V_{micro}/V_{total} ratio in the range 78.6-86.4% (comparable to 82.0% in BC). However, the SEM image of AB at a higher magnification displays an open network of large macropores in the size of 10-20 μm (Figure S2). The V_{micro}/V_{total} ratio of AB was 23.4% only, suggesting that the amino-modification was too chemically aggressive and resulted in the collapse of micropores and the development of a mesoporous structure, as illustrated in Figure 2. This was corroborated by the large average pore diameter of AB (4.85 nm) compared to the others (1.82-1.96 nm) in Table 1.

Based on the results of the Boehm's titration (Table 1), the chemically-modified biochars were found to have 0.703 to 2.359 mmol g^{-1} of surface acidic groups, which were 1.5 to 5.2 times of that of BC. The presence of carboxylic groups and phenolic groups on the biochars, and their changes as a result of chemical modifications, were confirmed by XPS spectra (Figure 3) and the corresponding elemental compositions (Table S1). The high-resolution C1s and O1s peaks were present on all biochars, whereas the N1s peaks only were displayed by BC, AB, and KB.

The deconvolution of C1s spectra revealed the presence of five component peaks (Figure 3), corresponding to graphitic carbon C=C or hydrocarbon C–C (Peak 1, 284.55-284.79 eV), carbon in phenol, alcohol C–O, C=N or CNH_2 (Peak 2, 285.64-286.04 eV), C=O bonds in carbonyl groups (Peak 3, 286.65-287.44 eV), O=C–O bonds in carboxyl or ester groups (Peak 4, 288.44-288.98 eV), and shake-up satellite peaks due to a π-π* transition in aromatic rings (Peak 5, 290.27-290.87 eV) (Georgiou et al., 2010; Yue et al., 1999). It was evident that

the specific surface areas of modified biochar reduced with increasing O-containing functional groups (i.e., C=O, O=C–O, C–O) (Table S2), or increasing oxygen content on the surfaces (Table S1).

The O1s spectra were resolved into four peaks (Figure S3): oxygen in carbonyl group C=O (Peak 1, 530.90-531.48 eV), oxygen in hydroxyl or ether groups C–O (Peak 2, 532.23-532.46 eV), oxygen in carboxyl or ester groups O=C–O (Peak 3, 533.21-533.50 eV), and chemisorbed oxygen or adsorbed water (Peak 4, 534.01-536.33 eV) (Georgiou et al., 2010; Walczyk et al., 2005; Yue et al., 1999). The N1s spectra of BC, KB, and AB were fitted into two individual peaks (Figure S4): C=N (Peak 1, 398.89-399.21 eV) and quaternary N or –NO groups (Peak 2, 400.79-401.11 eV) (Jansen et al., 1995; Reis et al., 1995; Singh et al., 2014). In comparison, nitrogen atoms in an amide or amine of ester (Peak 3, 399.71 eV) were found in the N1s spectra after amino-modification. These deconvoluted peaks, along with the increase in nitrogen content in the elemental composition (Table S1), indicated successful grafting of amino groups on the surface of AB after modification.

Thermogravimetric analysis (Figure S5a) showed that BC was the most thermally stable with 5% weight loss at ~345 ^{o}C, while the thermal stability of biochar deteriorated after the chemical modifications. It was noted that the temperatures corresponding to 5% weight loss in all chemically-modified biochars were below 100 ^{o}C (76 ^{o}C for SB, 57 ^{o}C for PB, 59 ^{o}C for KB, and 67 ^{o}C for AB), indicating the removal of moisture from the biochars. Compared to BC (3.4% of water content), there was a larger amount of adsorbed water in the SB, PB, KB, and AB (6.5-9.7%). Thus, an introduction of hydroxyl groups during chemical modifications altered the hydrophobic nature of the biochar to more hydrophilic.

There was an additional decomposition stage between 160 and 370 ^{o}C for AB, which may be attributed to decarboxylation of carboxylic groups (Anstey et al., 2016). The substantial weight loss above 350 ^{o}C may reflect the degradation of recalcitrant condensed

organic carbon (Chen and Huang, 2011) and conversion of carbon to CO, CO_2, and CH_4. There was an obvious shift of the broad peak at 600 ^oC to 560 ^oC for KB (Figure S5b), which may reflect the pore structure of the biochar was changed by KOH-modification, leading to a collapse of micropores (Table 1), and thus deteriorating the thermal stability. From 800 ^oC onwards, the degradation of lignocellulose substances in biochars was completed and the curves remained unchanged. The reduction in residual masses also indicated a decrease in thermal stability of the biochar after the studied chemical modifications.

3.2. Effects of modified biochars on E. coli retention and remobilization

The retention and remobilization of *E. coli* during intermittent infiltration cycles are illustrated in Figure 4. The viable counts of *E. coli* in the influent were measured before and after each infiltration cycle, and were maintained at a concentration of 10^6 CFU mL^{-1}, representing concentration on the high side of the reported range in stormwater (Lundy et al., 2012). All columns with biochar removed 92.1% to 98.7% of the total amount of *E. coli* injected in the entire storm event (Table 3). In contrast, the overall removal was only 35% in the sand column packed with AWS (90% by weight) and IOCS (10% by weight) (Table 3). The effluent bacterial concentrations generally increased with the continuous infiltration of bacteria-containing stormwater. In the second infiltration cycle, a small decrease in removal capacity (1.9-7.9%) was observed in SB, PB, and KB compared to the first infiltration cycle, while the reduction was slightly more notable in AB (10.8%) (Table 3). Hence, biochars showed promising *E. coli* removal capacities with low bacterial remobilization arising from intermittent rainfall events.

Bacterial adhesion can be explained by Derjaguin-Landau-Verwey-Overbeek (DLVO) theory (DeNovio et al., 2004; Hori & Matsumoto, 2010; van Loosdrecht et al., 1990). The degree of attraction between surfaces of bacteria and filter media is determined by the net

interaction potential due to attractive van der Waals and repulsive electrostatic interactions. Ionic strength reduction and pH increase can mobilize inorganic/organic colloids in both saturated and unsaturated porous systems due to an enhanced electrostatic repulsion (DeNovio et al., 2004). However, the increases in effluent pH attributed to additions of BC (pH 7.1) and KB (pH 8.5) did not lower the bacterial retention in biochar columns, while the effluent pH values in other columns (6.9 for PB, 6.8 for SB, 6.4 for AB) were comparable with or slightly lower than the sand column (pH 6.9). Therefore, other mechanisms, e.g., pore straining and hydrophobic attraction, may also account for the high *E. coli* deposition.

Although biochar also provides surface active sites for *E. coli* removal, the specific receptor-ligand interactions may be exhausted over time due to continuous bacterial loading in bioretention columns. The high removal efficiency of *E. coli* may be primarily attributed to the large surface area of biochars (113.8-230.6 m^2 g^{-1} given in Table 1, except AB) as compared to sand and IOCS (0.82 m^2 g^{-1}). Yet, it is noted that pore sizes of 2 to 5 times greater than the cell size are needed to maximize adhesion of microorganisms (Samonin and Elikova, 2004), hence the specific surface area includes internal pores of biochars that are not available for the attachment of *E. coli* (~0.8 μm diameter) (Pierucci, 1978).

The remobilization of attached *E. coli* from the biochar columns was marginal (0.2-2.0%) during gravitational drainage and intermittent flow (Table 3), while a greater fraction of deposited *E. coli* (4.6%) was mobilized from sand column despite its low removal during stormwater infiltration. The bacterial transport in intermittent flows was possibly driven by air-water interface scouring and induced shear force depending on the rainfall solution history and soil heterogeneity (DeNovio et al., 2004; Mohanty et al., 2016). Only a minimal amount of attached *E. coli* (0.04-0.33%) was eluted from biochar columns in the first gravitational drainage. However, in the KB and AB columns, *E. coli* remobilization increased substantially during the second gravitational drainage (1.43-4.44%). A net bacterial growth was less likely

during the 16-h pause in stationary phase (Finkel, 2006). Thus, the increase in bacterial remobilization for the succeeding infiltration cycle may reflect less bacterial deposition by straining due to loss of low-density biochar particles during intermittent flows (Mohanty and Boehm, 2015; Wang et al., 2013).

A high overall removal of *E. coli* (96.6%) was achieved by original biochar in the bioretention columns. The H_2SO_4 modification slightly increased the performance, especially for minimizing the bacteria remobilization (Figure 4), while H_3PO_4 and KOH modifications had little influence. In contrast, the amino-modified biochar, which has a high binding affinity for cationic contaminants, compromised the effectiveness of *E. coli* removal (92.1%) despite being far superior to that of the sand column (35%). Bacterial removal capacity appears to correlate with the surface area of biochar (Table 1) with linear correlation coefficient of 0.92. The porosity of biochars also plays a role in bacteria attachment. Despite its low surface area (2.63 m^2 g^{-1}), the original micropores within biochar were transformed into mesopores (4.85 nm) by amino-modification, which were more accessible and suitable for bacteria attachment. As a result, the retention of bacteria was still reasonably high although the attached bacteria in large pores were prone to remobilization as revealed in Figure 4.

In addition, surface hydrophobicity has been regarded as an important factor in bacterial adhesion because there is an increasing bacteria deposition on more hydrophobic surfaces (Faille et al., 2002; Kingshott et al., 2003; Rivera-Utrilla et al., 2001). The surface acidity of biochar was increased by all chemical modifications (Table 1), while in particular the O-containing functional groups were largely introduced to the biochar surface via amino-modification as revealed by XPS analysis (Table 2). This implies that the surface of AB became more hydrophilic due to a significant increase in density of polar groups, which accounted for the observation that AB was less favourable for removing hydrophobic bacteria

compared to other modified biochars.

Nevertheless, various bacterial strains such as *E. faecalis* (gram-positive) and *E. coli* (gram-negative) have been reported to display a varying extent of bacterial attachment (Faille et al., 2002; van Loosdrecht et al., 1987) and different retention mechanisms as well as transport behaviour in saturated and unsaturated porous media (Chen and Walker, 2012; Hijnen et al., 2005; Mohanty et al., 2013). Moreover, the stormwater runoff quality and infiltration-drainage flow patterns (i.e., cycle and duration) significantly vary depending on climate, season, catchment area, and land use. Further investigation of engineered bioretention systems with modified biochars at a pilot/field scale is required for verifying their long-term performance and service life taking into account bacterial growth, biochar aging, and co-existing inorganic/organic contaminants using real stormwater runoff.

4. Conclusions

In this paper we have shown that in bioretention systems using biochar filter media, chemical modifications using H_2SO_4, H_3PO_4, KOH, and amino group grafting changed the physical and chemical properties of the biochars, which influenced the bacterial removal from synthetic stormwater and subsequent remobilization due to intermittent flow. All biochars regardless of chemical modifications demonstrated excellent performance as filter media in the bioretention system, providing a high capacity for bacterial removal while alleviating the extent of remobilization under intermittent flow. The H_2SO_4-modification improved *E. coli* retention and minimized subsequent remobilization by provision of a large surface area, whereas H_3PO_4- and KOH-modifications had marginal effects. In contrast, amino-modification caused a drastic change in the physiochemical properties and resulted in less effective performance. The surface area, porosity, and surface hydrophobicity of the biochars were suggested to play a significant role in controlling the fate and transport of *E.*

362 *coli*. Pilot- or field-scale investigations are needed to evaluate the long-term performance of
363 engineered bioretention systems under various flow regimes using real stormwater runoff.
364
365 **Acknowledgement**
366 The authors appreciate the financial support from the Hong Kong Research Grants
367 Council (PolyU 538613 and 15222115) for this study. The corresponding author particularly
368 thanks the NSF Research Center ReNUWIt, Prof. Richard G. Luthy, and Dr. Sanjay K.
369 Mohanty at Stanford University for their knowledge and experience sharing during his
370 attachment as a visiting scholar in 2011-2013.
371
372 **References**
373 Abit, S.M., Bolster, C.H., Cai, P. & Walker, S.L. (2012). Influence of feedstock and pyrolysis
374 temperature of biochar amendments on transport of Escherichia coli in saturated and
375 unsaturated Soil. *Environmental Science & Technology,* 46, 8097-8105.
376 Ahmad, M., Lee, S.S., Al-Wabel, M., Tsang, D.C.W. & Ok, Y.S. (2016). Biochar-induced
377 changes in soil properties affected immobilization/mobilization of metals/metalloids in
378 contaminated soils. *Journal of Soils and Sediments,* doi: 10.1007/s11368-015-1339-4.
379 Anstey, A., Vivekanandhan, S., Rodriguez-Uribe, A., Misra, M. & Mohanty, A.K. (2016).
380 Oxidative acid treatment and characterization of new biocarbon from sustainable Miscanthus
381 biomass. *Science of the Total Environment*, 550, 241-247.
382 Arnone, R.D. & Walling, J.P. (2007). Waterborne pathogens in urban watersheds. *Journal of*
383 *Water Health*, 5, 149-162.
384 Beiyuan, J., Tsang, D.C.W., Ok, Y.S., Zhang, W., Yang, X., Baek, K. & Li, X.D. (2016).
385 Integrating EDDS-enhanced washing with low-cost stabilization of metal-contaminated soil
386 from an e-waste recycling site. *Chemosphere*, 159, 426-432.

387 Boehm, H.P. (1994). Some aspects of the surface chemistry of carbon blacks and other
388 carbons. *Carbon*, 32, 759-769.
389 Bolster, C.H. & Abit, S.M. (2012). Biochar pyrolyzed at two temperatures affects Escherichia
390 coli transport through a sandy soil. *Journal of Environmental Quality*, 41, 124-133.
391 Chen, B. & Huang, W. (2011). Effects of compositional heterogeneity and nanoporosity of
392 raw and treated biomass-generated soot on adsorption and absorption of organic
393 contaminants. *Environmental Pollution*, 159, 550-556.
394 Chen, G. & Walker, S.L. (2012). Fecal indicator bacteria transport and deposition in saturated
395 and unsaturated porous media. *Environmental Science & Technology*, 46, 8782-8790.
396 CIRIA. *The SuDS Manual* (Report No. C753). London: CIRIA
397 Civic Exchange. (2011). *Liquid Assets IIIA: Dongjiang Overloaded – 2011 Dongjiang*
398 *Expedition Report.* Hong Kong: Civic Exchange, Noble Group.
399 Davis, A.P., Hunt, W.F., Traver, R.G. & Clar, M. (2009). Bioretention technology: Overview
400 of current practice and future needs. *Journal of Environmental Engineering*, 135, 109-117.
401 DeNovio, N.M., Saiers, J.E. & Ryan, J.N. (2004). Colloid movement in unsaturated porous
402 media: Recent advances and future directions. *Vadose Zone Journal*, 3, 338-351.
403 Faille, C., Jullien, C., Fontaine, F., Bellon-Fontaine, M., Slomianny, C. & Benezech, T.
404 (2002). Adhesion of Bacillus spores and Escherichia coli cells to inert surfaces: role of
405 surface hydrophobicity. *Canadian Journal of Microbiology*, 48, 728-738.
406 Fang, S., Tsang, D.C.W., Zhou, F., Zhang, W. & Qiu, R. (2016). Stabilization of cationic and
407 anionic metal species in contaminated soils using sludge-derived biochar. *Chemosphere*, 149,
408 363-271.
409 Finkel, S.E. (2006). Long-term survival during stationary phase: evolution and the GASP
410 phenotype. *Nature Review Microbiology*, 4, 113-120.
411 Gaffield, S.J., Goo, R.L., Richards, L.A., & Richard, J.J. (2003). Public health effects of

412 inadequately managed stormwater runoff. *American Journal of Public Health,* 93, 1527-1533.
413 Grant, S.B., Saphores, J.D., Feldman, D.L., Hamilton, A.J., Fetcher, T.D., Cook, P.L.M.,
414 Stewardson, M., Sanders, B.F., Levin, L.A., Ambrose, R.F., Deletic, A., Brown, R., Jiang, S.
415 C., Rosso, D., Cooper, W.J., Marusic, I. (2012). Taking the "waste" out of "wastewater" for
416 human water security and ecosystem sustainability. *Science,* 337, 681-686.
417 Hijnen, W.A.M., Brouwer-Hanzens, A.J., Charles, K.J. & Medema, G.J. (2005). Transport of
418 MS2 Phage, Escherichia coli, Clostridium perfringens, Cryptosporidium parvum, and Giardia
419 intestinalis in a gravel and a sandy soil. *Environmental Science & Technology*, 39, 7860-7868.
420 HK DSD. (2013). *Stormwater Drainage Manual (with Eurocodes incorporated): Planning,*
421 *Design and Management*. Hong Kong: Drainage Services Department.
422 HK GBC (2014). Government Leadership: Taking a New Step towards Water Conservation.
423 *GreenMAG,* 8, 12-19, Green Building Council, Hong Kong.
424 HK WSD. (2016). *Annual Report 2014/15.* Water Supplies Department, Hong Kong
425 Government.
426 Hori, K. & Matsumotob S. (2010). Bacterial adhesion: From mechanism to control.
427 *Biochemical Engineering Journal*, 48, 424-434.
428 Jansen, R.J.J. & Bekkum, H.V. (1995). XPS of nitrogen-containing functional groups on
429 activated carbon. *Carbon*, 33, 1021-1027.
430 Kang, K., Gou, Z., Zhang, J., Xie, H., Liu, H. & Zhang, C. (2016). Enhancement of Ni(II)
431 removal by urea-modified activated carbon derived from *Pennisetum alopecuroides* with
432 phosphoric acid activation. *Journal of the Taiwan Institute of Chemical Engineers,* 60, 335-
433 341.
434 Kingshott, P., Wei, J., Bagge-Ravn, D., Gadegaard, N. & Gram, L. (2003). Covalent
435 attachment of poly(ethylene glycol) to surfaces, critical for reducing bacterial adhesion.
436 *Langmuir*, 19, 6912-6921.

437 Li, K., Li, J., Lu, M., Li, H. & Wang, X. (2016). Preparation and amino modification of
438 mesoporous carbon from bagasse via microwaveactivation and ethylenediamine
439 polymerization for Pb(II) adsorption. *Desalination and Water Treatment*, available online,
440 doi: dx.doi.org/10.1080/19443994.2016.1138891.
441 Lim, K.Y., Hamilton, A.J. & Jiang, S.C. (2015). Assessment of public health risk associated
442 with viral contamination in harvested urban stormwater for domestic applications. *Science of*
443 *the Total Environment,* 523, 95-108.
444 Lin, Y., Munroe, P., Joseph, S, Henderson, R. & Ziolkowski, A. (2012). Water extractable
445 organic carbon in untreated and chemical treated biochars. *Chemosphere,* 87, 151-157.
446 Liu, M.Y., Tsang, D.C.W., Hu, J., Ng, K.T.W., Liu, T., & Lo, I.M.C. (2008). Adsorption of
447 methylene blue and phenol by wood waste derived activated carbon. *Journal of*
448 *Environmental Engineering,* 134, 338-345.
449 Liu, P., Liu, W.J., Jiang, H., Chen, J.J., Li, W.W. & Yu, H.Q. (2012). Modification of bio-
450 char derived from fast pyrolysis of biomass and its application in removal of tetracycline
451 from aqueous solution. *Bioresource Technology,* 121, 235-240.
452 Lundy, L., Ellis, J.B. & Revitt, D.M. (2012). Risk prioritisation of stormwater pollutant
453 sources. *Water Research,* 46, 6589-6600.
454 Mohanty, S.K. & Boehm, A.B. (2015). Effect of weathering on mobilization of biochar
455 particles and bacterial removal in a stormwater biofilter. *Water Research,* 85, 208-215.
456 Mohanty, S.K., Cantrell, K.B., Nelson, K.L., & Boehm, A.B. (2014). Efficacy of biochar to
457 remove *Escherichia* coli from stormwater under steady and intermittent flow. *Water*
458 *Research,* 61, 288-296.
459 Mohanty, S.K., Saiers, J.E., Ryan, J.N. (2016). Colloid mobilization in a fractured soil: Effect
460 of pore-water exchange between preferential flow paths and soil matrix. *Environmental*
461 *Science & Technology,* 50, 2310-2317.

462 Mohanty, S.K., Torkelson, A., Dodd, H., Nelson, K., & Boehm, A. (2013). Engineering
463 solutions to improve the removal of fecal indicator bacteria by bioinfiltration systems during
464 intermittent flow of stormwater. *Environmental Science & Technology,* 47, 10791-10798.
465 Pierucci, O. (1978). Dimensions of Escherichia coli at Various Growth Rates: Model for
466 Envelope Growth. *Journal of Bacteriology,* 135, 559-574.
467 Rajapaksha, A.U., Vithanage, M., Lee, S.S., Seo, D.C., Tsang, D.C.W. & Ok, Y.S. (2016b).
468 Steam activation of biochars facilitates kinetics and pH-resilience of sulfamethazine sorption.
469 *Journal of Soils and Sediments,* 16, 889-895.
470 Rajapakshaa, A.U, Chen, S.S., Tsang, D.C.W., Zhang, M., Vithanage, M., Mandal, S., Gao,
471 B., Bolan, N.S. & Ok, Y.S. (2016a). Engineered/designer biochar for contaminant
472 removal/immobilization from soil and water: Potential and implication of biochar
473 modification. *Chemosphere,* 148, 276-291.
474 Rivera-Utrilla, J., Bautista-Toledo, I., Ferro-García, M.A. & Moreno-Castilla C. (2001).
475 Activated carbon surface modifications by adsorption of bacteria and their effect on aqueous
476 lead adsorption. *Journal of Chemical Technology and Biotechnology,* 76, 1209-1215.
477 Roy-Poirier, A., Champagne, P. & Filion, Y. (2010). Review of bioretention system research
478 and design: Past, present, and future. *Journal of Environmental Engineering,* 136, 878-889.
479 Samonin, V.V. & Elikova, E.E. (2004). A study of the adsorption of bacterial cells on porous
480 materials. *Microbiology,* 73, 696-701.
481 Singh, B., Fang, Y., Cowie, B.C.C. & Thomsen, L. (2014). NEXAFS and XPS
482 characterisation of carbon functional groups of fresh and aged biochars. *Organic*
483 *Geochemistry,* 77, 1-10.
484 Stagge, J.H., Davis, A.P., Jamil, E. & Kim, H. (2012). Performance of grass swales for
485 improving water quality from highway runoff. *Water Research,* 46, 6731-6742.
486 Takagagi, T. & Ishitani, A. (1984). XPS studies by use of the digital difference spectrum

technique of functional groups on the surface of carbon fiber. *Carbon,* 22, 43-46.

Tsang, D.C.W., Hu, J., Liu, M.Y., Zhang, W., Lai, K.C.K. & Lo, I.M.C. (2007). Activated carbon produced from waste wood pallets: Adsorption of three classes of dyes. *Water, Air, and Soil Pollution,* 184, 141-155.

van Loosdrecht, M.C., Lyklema, J., Norde, W. & Zehnder, A.J. (1990). Influence of interfaces on microbial activity. *Microbiological Reviews,* 54, 75-87.

van Loosdrecht, M.C., Lyklema, J., Norde, W., Schraa, G, & Zehnder, A.J. (1987). The role of bacterial cell wall hydrophobicity in adhesion. *Applied and Environmental Microbiology,* 53, 1893-1897.

Walczyk, M., Świątkowski, A., Pakuła, M. & Biniak, S. (2005). Electrochemical studies of the interaction between a modified activated carbon surface and heavy metal ions. *Journal of Applied Electrochemistry,* 35, 123-130.

Wang, D., Zhang, W., Hao, X. & Zhou, D. (2013). Transport of biochar particles in saturated granular media: Effects of pyrolysis temperature and particle size. *Environmental Science & Technology,* 47, 821-828.

Water by Design. (2014). *Bioretention Technical Design Guidelines.* Brisbane: Healthy Waterways Ltd.

Yang, G. X. & Jiang, H. (2014). Amino modification of biochar for enhanced adsorption of copper ions from synthetic wastewater. *Water research,* 48, 396-405.

Yue, Z.R., Jiang, W., Wang, L., Gardner, S.D. & Pittman Jr., C.U. (1999). Surface characterization of electrochemically oxidized carbon fibers. *Carbon,* 37, 1785-1796.

Zhang, W., Zheng, J., Zheng, P., Tsang, D.C.W. & Qiu, R. (2015). Sludge-derived biochar for As(III) immobilization: Effects of solution chemistry on sorption behavior. *Journal of Environmental Quality,* 44, 1119-1126.

(a)

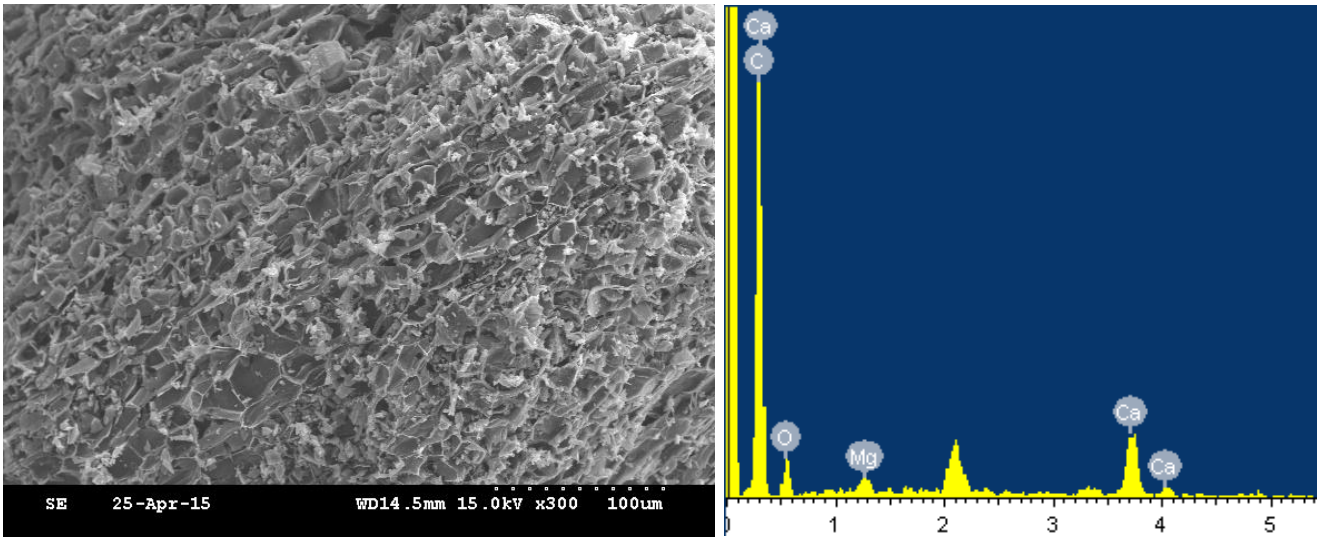
SE 25-Apr-15 WD14.5mm 15.0kV x300 100um
Ca
C
O
Mg
Ca
Ca
0
1
2
3
4
5

(b)

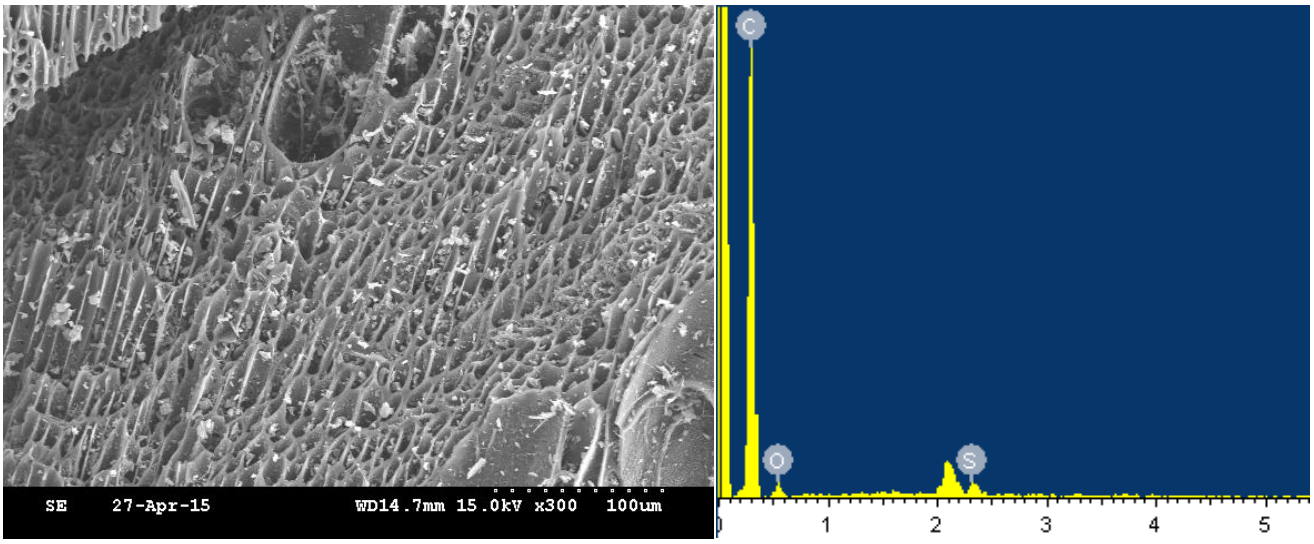
SE 27-Apr-15 WD14.7mm 15.0kV x300 100um
C
O
S
0
1
2
3
4
5

(c)

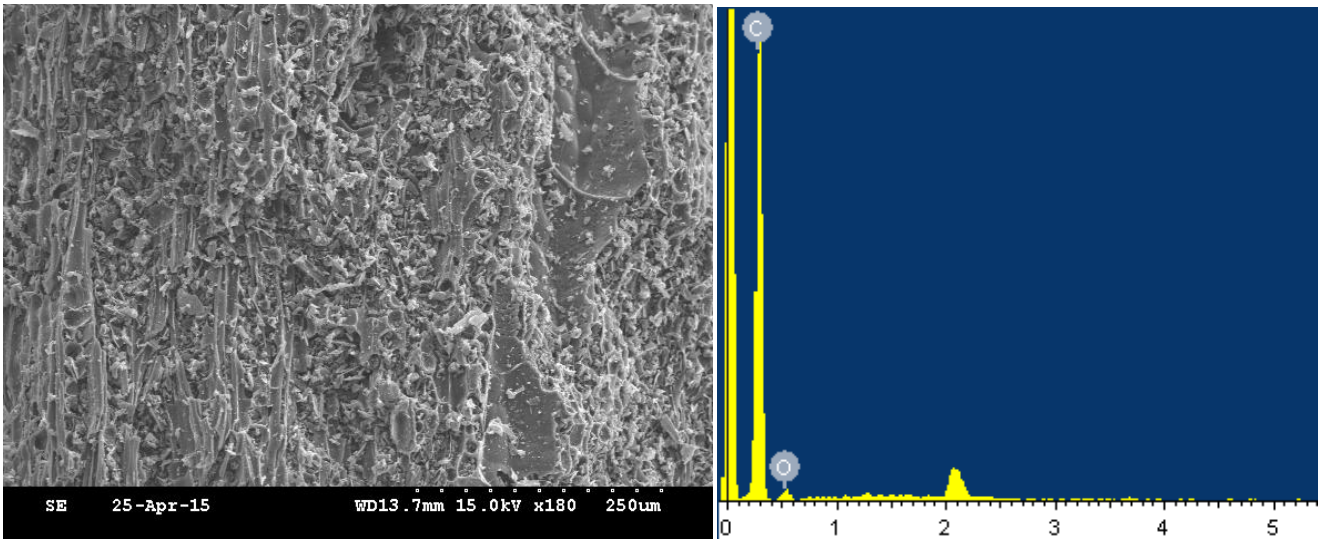
SE 25-Apr-15 WD13.7mm 15.0kV x180 250um
C
O
0
1
2
3
4
5

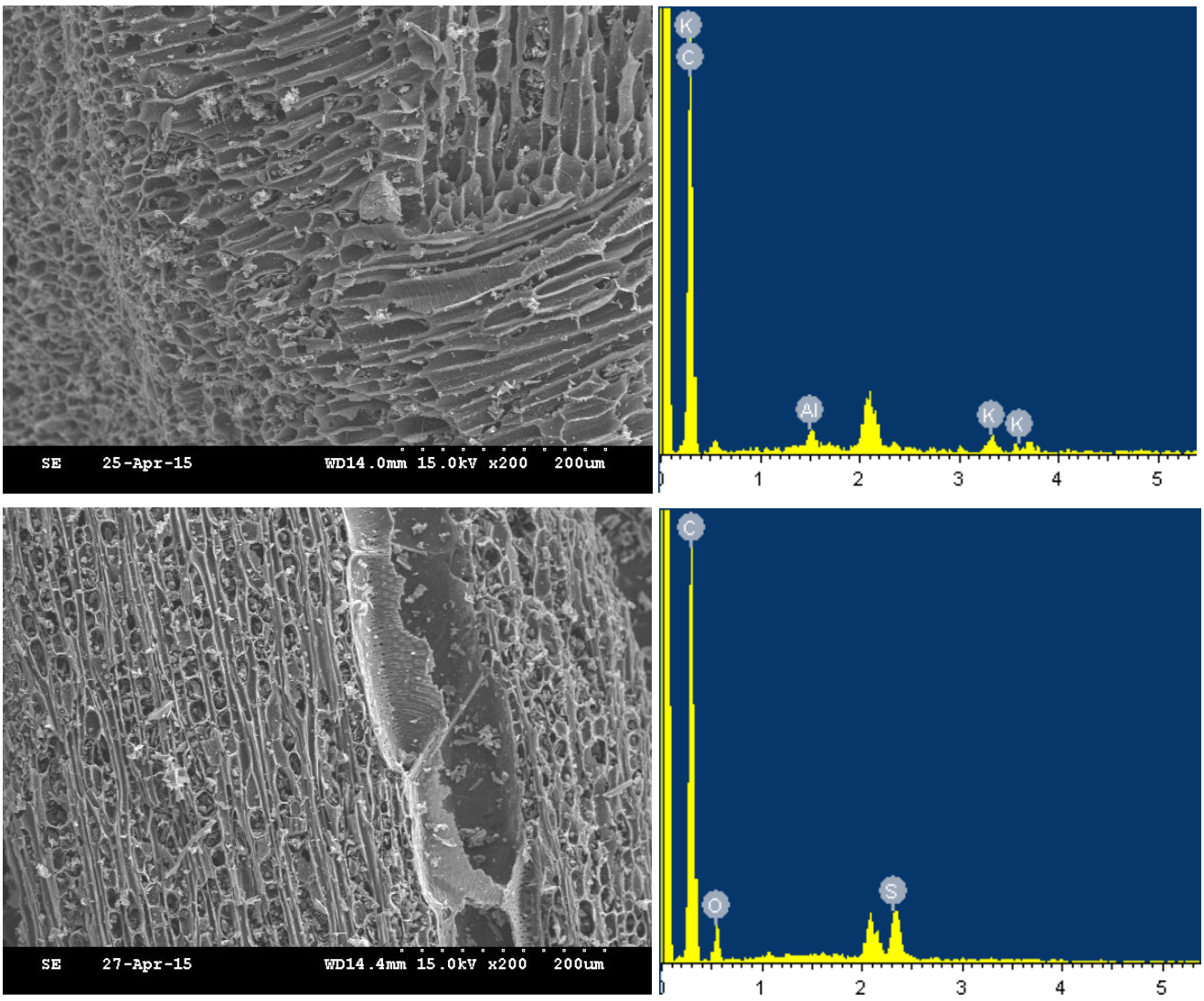

Figure 1. SEM images and corresponding EDS spectra of: (a) BC, (b) SB, (c) PB, (d) KB, and (e) AB (BC: original biochar, SB: H_2SO_4-modified biochar, PB: H_3PO_4-modified biochar, KB: KOH-modified biochar, and AB: amino-modified biochar).

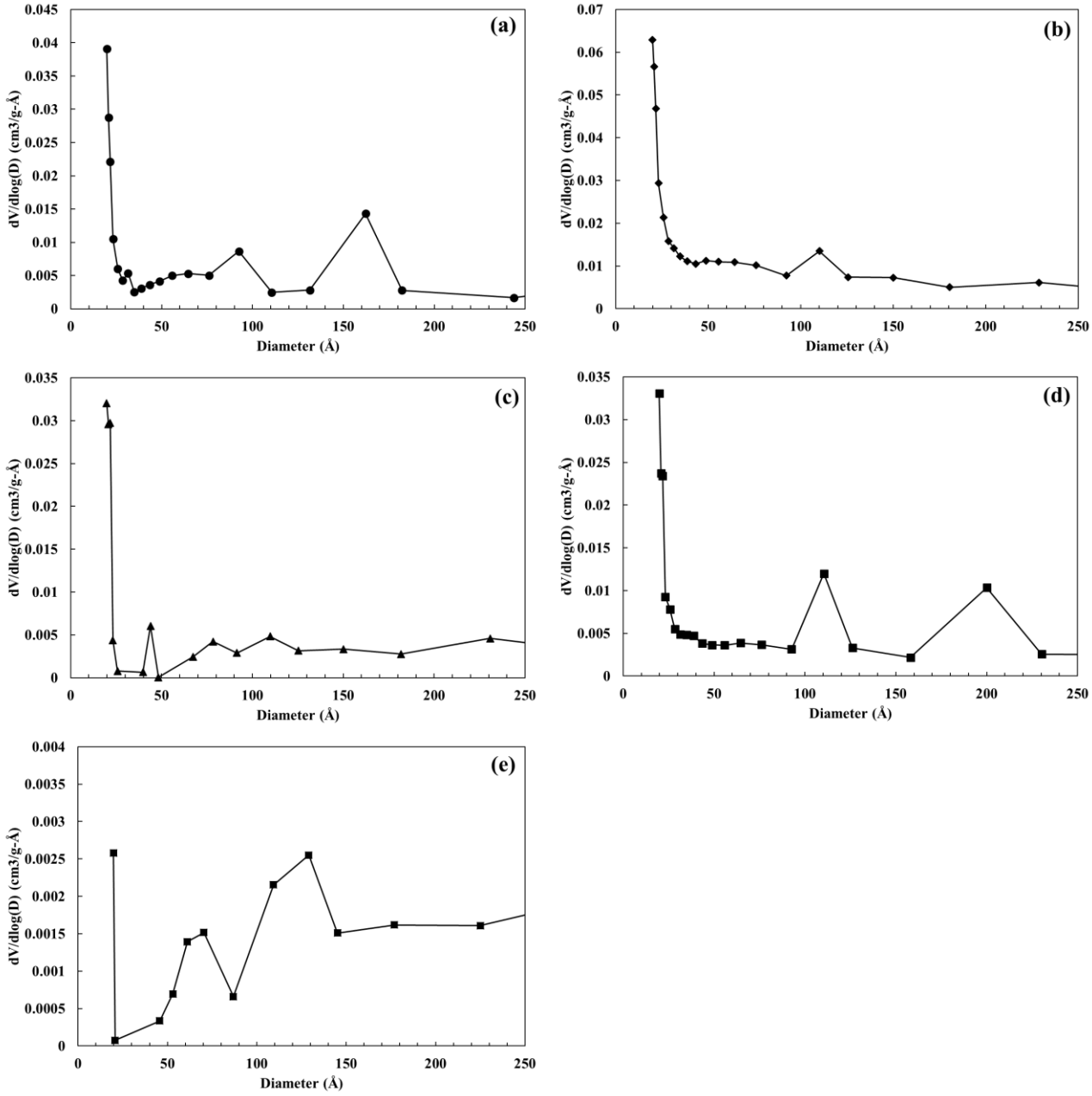

Figure 2. Pore size distribution of: (a) BC, (b) SB, (c) PB, (d) KB, and (e) AB (BC: original biochar, SB: H_2SO_4-modified biochar, PB: H_3PO_4-modified biochar, KB: KOH-modified biochar, and AB: amino-modified biochar).

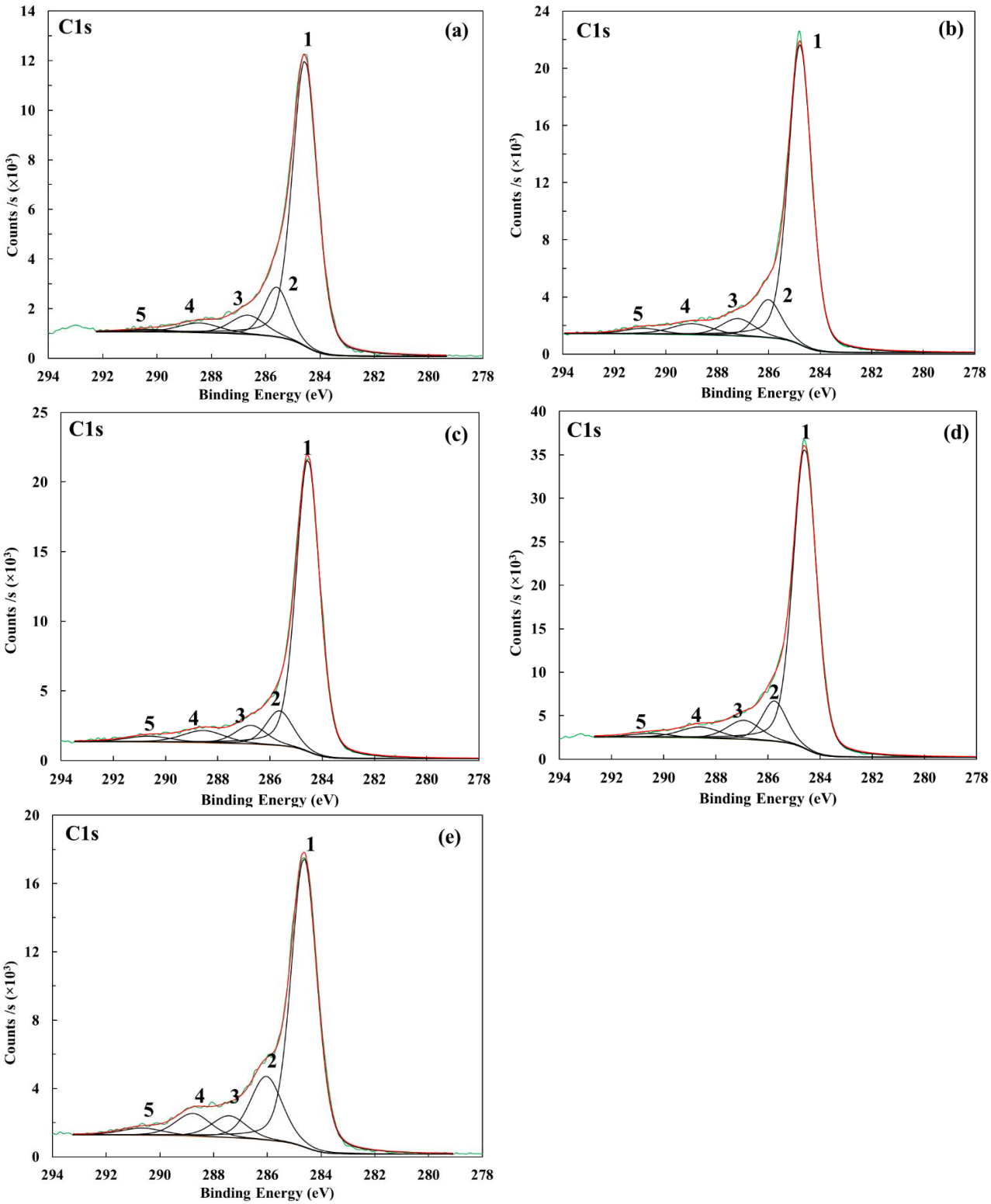

Figure 3. High-resolution XPS C1s spectra of: (a) BC, (b) SB, (c) PB, (d) KB, and (e) AB (Peak 1: C=C or C–C, Peak 2: C–O, C=N or CNH_2; Peak 3: C=O; Peak 4: O=C–O; and Peak 5: π-π* transition; BC: original biochar, SB: H_2SO_4-modified biochar, PB: H_3PO_4-modified biochar, KB: KOH-modified biochar, and AB: amino-modified biochar).

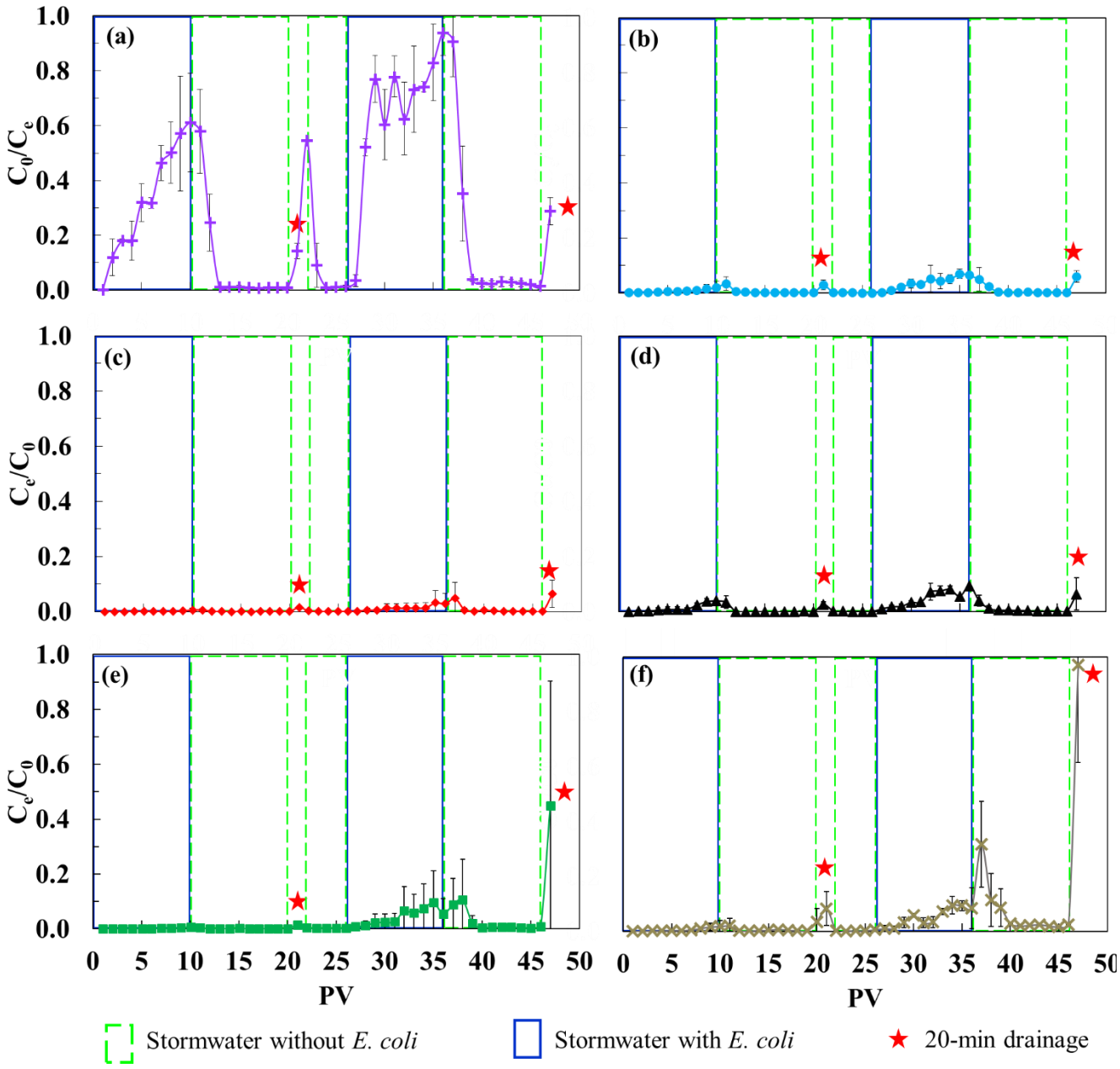

Figure 4. Breakthrough curves for *E. coli* in bioretention columns containing: (a) IOCS, (b) BC, (c) SB, (d) PB, (e) KB, and (f) AB (blue solid lines: injection of stormwater with *E. coli* (1-10 PV and 27-36 PV); green dotted lines: injection of stormwater without *E. coli* (11-20 PV, 22-26 PV, and 37-46 PV); red stars: 20-min gravitational drainage after infiltration (21 PV and 47 PV); biochar was blended with sand at 5% by weight; IOCS: iron oxide-coated sand; BC: original biochar, SB: H_2SO_4-modified biochar, PB: H_3PO_4-modified biochar, KB: KOH-modified biochar, and AB: amino-modified biochar).

Table 1. Physicochemical characteristics of original and modified biochars.

Physical Properties	**BC**	**SB**	**PB**	**KB**	**AB**
BET surface area, S_{BET} (m^2 g^{-1})	137.0	230.6	160.9	113.8	2.63
Micropore surface area, S_{micro} (m^2 g^{-1})	121.9	198.9	145.9	99.8	1.69
External surface area, S_{ext} (m^2 g^{-1})	15.1	31.6	14.9	14.0	0.94
Total pore volume, V_{total} (m^3 g^{-1})	0.0622	0.1052	0.0733	0.0557	0.0032
Mircopore volume, V_{micro} (m^3 g^{-1})	0.0510	0.0827	0.0633	0.0450	0.0007
V_{micro}/V_{total} (%)	82.0	78.6	86.4	80.7	23.4
Average pore diameter, D_p (nm)	1.82	1.82	1.82	1.96	4.85
Chemical Characteristics	**BC**	**SB**	**PB**	**KB**	**AB**
Basicity (mmol g^{-1})	1.015	0.048	0.905	0.897	0.069
Acidity (mmol g^{-1})	0.456	0.703	2.359	0.830	1.474
Carboxylic groups (mmol g^{-1})	0.116	0.240	1.646	0.313	0.606
Lactonic groups (mmol g^{-1})	N.D.	N.D.	N.D.	N.D.	N.D.
Phenolic groups (mmol g^{-1})	0.340	0.463	0.713	0.517	0.868

N.D.: not detectable; BC: original biochar, SB: H_2SO_4-modified biochar, PB: H_3PO_4-modified biochar, KB: KOH-modified biochar, and AB: amino-modified biochar.

Table 2. Distribution of surface functional groups (%) of original and modified biochars.

Biochars	C=C / C–C	C-O	C=O	O=C–O	π-π* transition
BC	74.9	13.0	6.9	4.2	0.9
SB	75.7	10.6	6.4	5.0	2.4
PB	75.0	10.0	6.3	5.7	2.9
KB	76.1	10.6	6.8	4.7	1.8
AB	65.6	18.1	6.7	6.9	2.7

BC: pristine biochar, SB: H_2SO_4-modified biochar, PB: H_3PO_4-modified biochar, KB: KOH-modified biochar, and AB: amino-modified biochar.

Table 3. *E. coli* removal and remobilization in bioretention columns containing different biochars (5% w/w) during the entire flow regime (i.e., two infiltration cycles and two gravitational drainages with intermittent flow).

Column	*E. coli* removal (%)			*E. coli* remobilization (%)		
	1st Infiltration Cycle [a]	2nd Infiltration Cycle [a]	Overall [b]	1st Drainage [c]	2nd Drainage [c]	Intermittent Flow [d]
IOCS	54.6	29.3	35.0	1.30	7.06	12.09
BC	98.9	96.8	96.6	0.12	0.24	0.04
SB	99.8	97.9	98.7	0.05	0.28	0.04
PB	98.2	94.1	96.0	0.11	0.29	0.09
KB	99.7	92.8	96.4	0.04	1.43	0.11
AB	98.6	87.9	92.1	0.33	4.44	0.11

[a] Percentage of total *E. coli* attached in the infiltration cycles (i.e., 1-20 PV and 22-46 PV before drainage by gravity);
[b] Percentage of total *E. coli* attached (i.e., 1-47 PV);
[c] Percentage of total *E. coli* detached during gravitational drainages (i.e., 21 PV and 47 PV);
[d] Percentage of total *E. coli* detached during intermittent flow (i.e., 22-26 PV).
IOCS: iron oxide-coated sand; BC: original biochar, SB: H_2SO_4-modified biochar, PB: H_3PO_4-modified biochar, KB: KOH-modified biochar, and AB: amino-modified biochar.

Supplementary Material

Click here to download Supplementary Material: CHEM_BC_SI_DT.DOCX